Nuclear Engineering and Design 419 (2024) 112992

Contents lists available at ScienceDirect

Nuclear Engineering and Design

journal homepage: www.elsevier.com/locate/nucengdes

On the behavior of a concrete-based dry cask for spent nuclear fuel in off-normal and accidental conditions

Michela Angelucci [a,*], Luis E. Herranz [b], Sandro Paci [a]

[a] Department of Industrial and Civil Engineering, University of Pisa (UNIPI), 56122 Pisa, Italy
[b] Centro de Investigaciones Energeticas, Medioambientales y Tecnológicas (CIEMAT), 28040 Madrid, Spain

ARTICLE INFO

Keywords:
Dry cask
Spent fuel
Off-normal conditions
Accidental conditions
MELCOR
Nuclear safety

ABSTRACT

The safe storage of Spent Nuclear Fuel (SNF) within a dry cask system must be guaranteed for any operating condition. In particular, the Peak Cladding Temperature (PCT) is currently employed as a measure of the fuel integrity in normal conditions. The same fuel integrity has to be ensured also in off-normal and accidental conditions by keeping the PCT below the regulatory limits. In this regard, the work proposed in this paper aims at evaluating the performance of a concrete-based dry cask in off-normal and accidental conditions. More specifically, the influence of a partial to complete blockage of the air inlet openings on the PCT is assessed by means of a MELCOR model of the HI-STORM 100S cask. Attention is also paid to the temperature of the external concrete cask in order to check the integrity of the concrete itself.

1. Introduction

Dry Cask Systems (DCSs) have proven to be a good option for the interim storage of Spent Nuclear Fuel (SNF) and a valid alternative to wet storage systems such as Spent Fuel Pools (SFPs) (IAEA, 2002; Bunn et al., 2001).

As the name implies, DCSs are characterized by the storing of the SNF in a dry and inert environment. Cooling is ensured by natural convection, and the unnecessariness of any ventilation system and of electrical supply makes DCSs also passive. Moreover, their extreme flexibility as well as their modularity promotes an efficient and cost-effective SNF management and allows them to adapt to circumstances changing over time.

Along with the appealing features mentioned above, DCSs are meant to show consistency with the safety requirements as codified in the Code of Federal Regulation (CFR) under 10CFR72 (U.S. NRC). In particular, fuel integrity should be maintained.

Considering the temperature-dependent nature of most degradation-related mechanisms, a great deal of attention has been devoted to the thermal characterization of DCSs in the past decades. Simulations aimed at reproducing the thermal state of several types of dry casks have been carried out using different classes of codes. In the 80's, thermal–hydraulic codes, such as COBRA-SFS (Rector et al., 1986) and HYDRA (Nourgaliev et al., 2013), were employed for the purpose. These codes were based on a control-volume approach, but their reliability was lessened by the over-simplification of energy and momentum equations. The need to overcome this issue together with the increasing availability of computational power led, later on, to the employment of Computational Fluid Dynamics (CFD) codes, such as STAR CCM+ (SIEMENS), CFX (Ansys Inc), and FLUENT (Ansys Inc.), able to reach a higher level of accuracy and preciseness, but at the expense of the computational time. To the date, CFD simulations are by far the reference method to obtain insights into the thermal behavior of the cask itself and of the SNF contained in it, as proven by the amount of studies carried out in the past few years (Benavides et al., 2019; Herranz et al., 2015; U.S. NRC, 2013; Wang et al., 2021; Wu et al., 2018). However, more recently, studies have proved that the general performance of the entire DCS can be also represented through simpler (Penalva et al., 2021) and faster (Angelucci et al., 2021) approaches, particularly if the target is the so-called Peak Clad Temperature (PCT) and not the full thermal characterization of the cask.

Despite the number of investigations about DCSs, very few of them explore their behavior in off-normal or accidental conditions, the high computation cost being one of the main reasons for it. In (Šimonis et al., 2013) the thermal analysis, through the ALGOR code, of the CONSTOR RBMK 1500/M2 cask (Poskas et al., 2006) at the Ignalina Nuclear Power Plant (NPP) is carried out. Normal operating conditions as well as abnormal ones (such as helium leakage, erroneous loading, and half-

* Corresponding author.
E-mail address: michela.angelucci@unipi.it (M. Angelucci).

https://doi.org/10.1016/j.nucengdes.2024.112992
Received 7 November 2023; Received in revised form 7 January 2024; Accepted 2 February 2024

blockage of the ventilation system) are considered. Helium leakage is also studied in (Penalva et al., 2017), where both CFD calculations and a more mathematical approach are employed to characterize the SNF thermal response to a postulated canister depressurization in a concrete-based dry cask. In (Lee et al., 2005) the thermal performance of a ventilated concrete cask for 24 Pressurized Water Reactor (PWR) spent Fuel Assemblies (FAs) is assessed by using the FLUENT code, and results are compared against experimental data (Bang et al., 2014). A similar work has been performed in (Li and Liu, 2016), where the complete blockage of the air inlets is studied as well. In (Ratiko et al., 2022), instead, the heat removal by means of natural airflow is evaluated for a prototypical DCS for a Material Testing Reactor (MTR) spent fuel. Both theoretical and experimental results are presented, and the closing of the air vents is also investigated.

In this framework, taking into account that the safe storage of SNF within a DCS must be guaranteed for any operating condition, the present paper aims at evaluating the performance of a concrete-based DCS in off-normal and accidental conditions. More specifically, the influence of a partial to complete blockage of the air inlet openings on the PCT, which is the variable under regulatory surveillance, is assessed for the HI-STORM 100S system (HOLTEC, 2010). Attention is also paid to the temperature of external concrete cask, which has to maintain its integrity and its shielding role.

The present investigation adds up to the quite limited number of studies available in the literature. However, unlike prior efforts mainly relying on CFD calculations, this work explore the thermal performance of DCSs, in scenarios other than normal operating conditions, by means of a system code. More precisely, this is the first application of a system code for the purpose.

In particular, the MELCOR code, version 2.2.18019 (Humphries et al., 2021; Humphries et al., 2021), has been employed to carry out the analysis. The choice is motivated primarily by MELCOR proven ability to reproduce the thermal behavior of the HI-STORM 100S system both in normal operating condition (Angelucci et al., 2021) and under more challenging boundary conditions (such as higher decay power and hotter external air temperature) (Angelucci et al., 2022). In addition, the use of MELCOR introduces a significant reduction in the computational time, with an enhanced efficiency of the analysis itself.

As a further step, an additional scope can be defined for the present study: testing the MELCOR code outside its natural domain of application. In fact, while conventionally recognized as a reference code for modelling the progression of a Severe Accident (SA), confirming its flexibility and versatility may broaden the spectrum of application of this already powerful tool.

2. System and scenario

The HI-STORM 100S is a storage system for SNF, that consists of two main components (Fig. 1): a metallic cask, called Multi-Purpose Canister (MPC), and a concrete overpack, in which the MPC is placed. The SNF is located within the sealed MPC (Fig. 2) shows the distribution of the FAs within the MPC).

The entire system is designed in full compliance with the requirements of 10CFR72 (U.S. NRC): confinement, radiation shielding, criticality control and passive heat removal.

Confinement is assured by the MPC structure: during storage, the SNF is enclosed in an enclosure vessel, whose boundaries are defined by the baseplate, the canister shell, the upper lid and the closure ring. No carbon steel parts are allowed in the canister, the components of which are made of long-term corrosion-resistant stainless steel alloys.

The shielding function is, instead, fulfilled by the thick concrete walls of the overpack, which provides also for the physical protection of

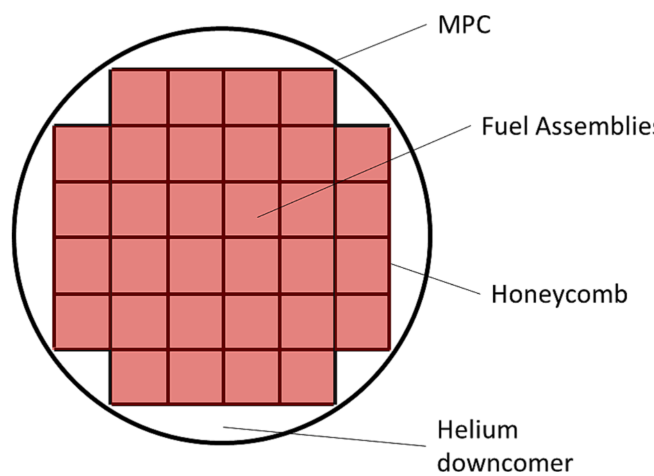

Fig. 2. Conceptual sketch of the MPC – top view.

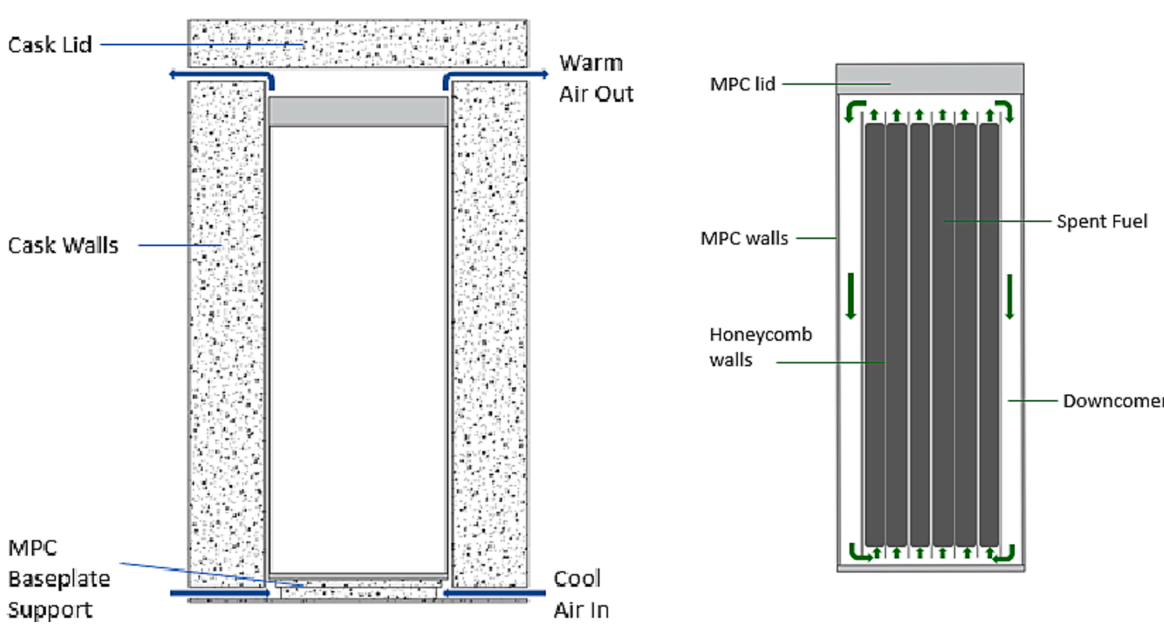

Fig. 1. Conceptual sketch of the HI-STORM 100S system.

both the canister and the fuel inside it. Contrarily to the MPC, the overpack does not constitute a confinement enclosure: four inlet and four outlet openings are located near the lower and upper extremities of the overpack to provide a passive natural convection cooling to the MPC. Openings are equipped with shield plates and a screen to provide additional radial shielding.

Criticality control has to be established in order to maintain a multiplication factor k-effective lower than 0.95 under normal, off-normal and accidental conditions. The geometry and the neutron absorbing materials in the MPC are the only measures necessary to reach this goal.

As for passive heat removal, two main mechanisms are involved, one within the MPC and one outside it. Within the canister, the atmosphere of which is pressurized and filled with 99.995 % pure Helium as backfill gas, the Helium flow is driven by natural convection in upward direction around the FAs and in downward direction next to the canister walls. This mechanism is known as thermosiphon effect.

Outside the MPC, instead, the cooling is mainly led by the natural circulation of the external air flowing in the air gap between the internal MPC and the external overpack. In addition to the processes mentioned above, radiative heat exchange from the MPC to the overpack also contributes to the heat removal.

Main dimensions of the HI-STORM 100S system are reported in Table 1.

For the analysis performed in this work, the considered canister is the MPC-32, equipped with 32 PWR 17x17 intact FAs (as shown in Fig. 2). The FAs have been considered equally powered, with no regionalization within the MPC. The total decay power has been imposed equal to 30.0 kW, in accordance with the design limits for the considered MPC (namely, MPC-32) (HOLTEC, 2010). It is worth underlying that to the aim of the present analysis, the definition of the decay power is enough for the evaluation of the thermal state of the system.

Furthermore, initial and boundary conditions to reach the steady state have been imposed as in (Herranz et al., 2015).

The thermal evaluation has been then carried out taking into account different scenarios, under off-normal and accidental conditions. As for the former, a partial blockage of the air inlets has been studied, considering 3 scenarios with growing severity:

- 1 inlet opening blocked, 3 open (corresponding to 75 % of the inlet area available);
- 2 inlet openings blocked, 2 open (corresponding to 50 % of the inlet area available);
- 3 inlet openings blocked, 1 open (corresponding to 25 % of the inlet area available).

As for the accidental scenario, a complete blockage has been considered, with all 4 inlet openings closed.

In addition, to further extend the thermal and safety assessment, an adiabatic case has been carried out. Albeit considered a bounding condition in the NUREG-1536 (U.S. NRC, 2010), it is worth exploring this extreme scenario to gather information on temperatures escalation and to identify the right timing for accident management.

Table 1
Main dimension of the HI-STORM 100S system (HOLTEC, 2010).

MPC	
Height (m)	4.85
Diameter (m)	1.78
Wall Thickness (m)	0.013
Baseplate Thickness (m)	0.06
Lid Thickness (m)	0.29
Overpack	
Height (m)	5.824
Diameter (m)	3.37
Wall Thickness (m)	0.75 *
Lid Thickness (m)	0.48
Baseplate Thickness (m)	0.124
MPC Support Thickness (m)	0.76
MPC Support Diameter (m)	1.65

*The cylindrical walls of the overpack are composed of a 0.70 m thick concrete wall enclosed in two 0.025 m thick layers of stainless steel.

3. MELCOR model

The HI-STORM 100S system has been modeled in its entirety with the MELCOR code (version 2.2) (Humphries et al., 2021; Humphries et al., 2021). In particular, the MELCOR model employed in this work for the reproduction of off-normal and accidental scenarios is an adaptation of a model previously developed for a steady state analysis and verified against a CFD model of the same system (the results of which were previously verified against data available in (HOLTEC, 2010)). The complete description of the initial MELCOR model for the HI-STORM 100S is given in (Angelucci et al., 2021, 2022). However, in view of the focus of the analysis, a brief description of the developed nodalization is given below, with particular attention to the annular air channel (in between the MPC and the overpack) and to the means to extract heat from the MPC containing the SNF.

To model the MPC internals, two distinct but interacting nodalizations have been implemented. The first one is mandated by the MELCOR CORe (COR) package, and it is fundamental to track the thermal response of the SNF. To do so, radial rings (4) and axial levels (12) have been defined so to mirror the characteristics of the region within the MPC, containing the fuel. On the other hand, the second nodalization is tailored to capture the thermal-hydraulics of the gas region. Specifically, 24 Control Volumes (CVs) and 26 Flow Paths (FPs) have been employed to reproduce the Helium flowing around the FAs within the MPC.

For the definition of the air channel between the canister and the overpack, instead, eight CVs have been employed, as shown in Fig. 3 (a). The CVs have been then connected by means of 9 FPs, 7 of which reproduce the vertical air flow in the annular gap (Fig. 3 (b)). The remaining two FPs represent, instead, the inlet and outlet openings connecting the annular gap with the external environment. Even if, in the actual cask, the openings are 8 (4 for the air inlet and 4 for the outlet), in the model the opening flow areas and the length of the junctions are merged in just 2 FPs: one for the incoming air and one for the outcoming. It is worth noting that this choice is related to the axy-simmetric nature of the model. In fact, the entire thermal–hydraulic nodalization for the air channel is the result of a compromise between three main factors: the correct reproduction of the behavior of the system, the lumped parameter nature of the MELCOR code and the computational time.

As for the walls of both the MPC and the overpack, the Heat Structure (HS) package in MELCOR has been used for their modeling. In particular, the MPC walls have been modeled with 14 HSs: 6 simulating the cylindrical part of the canister, 4 for the lid and 4 for the base (Fig. 4 (a)). All MPC structures are made of stainless steel, whose properties are implemented directly into MELCOR. On the other side, the walls of the overpack have been modeled with 11 HSs: 8 cylindrical HSs for the vertical structure, and 3 rectangular ones (1 for the lid, 1 for the baseplate, and 1 for the MPC support) (Fig. 4 (b)). In this case, the structures are made of METCON^{TM}, with a thick heart of concrete surrounded by 2 thin layers of carbon steel.

Whilst the Heat Transfer Coefficient (HTC) for the convective heat exchange between the HSs and the air is automatically calculated by the MELCOR code itself, the radiative exchange between the external wall side of the MPC and the internal wall side of the overpack has been taken into account with the activation of the so called structure-to-structure model. Considering the small width of the annular channel, view factors equal to 1.0 have been imposed for facing pairs of HSs. In addition, carbon and stainless steel emissivities have been user-imposed as in (Herranz et al., 2015).

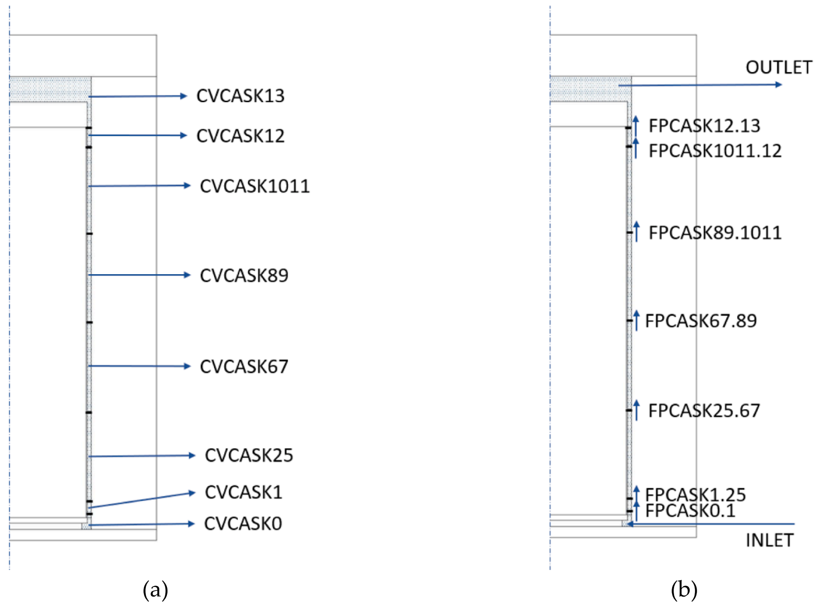

Fig. 3. Control volumes (a) and flow paths (b) employed in the nodalization of the air channel.

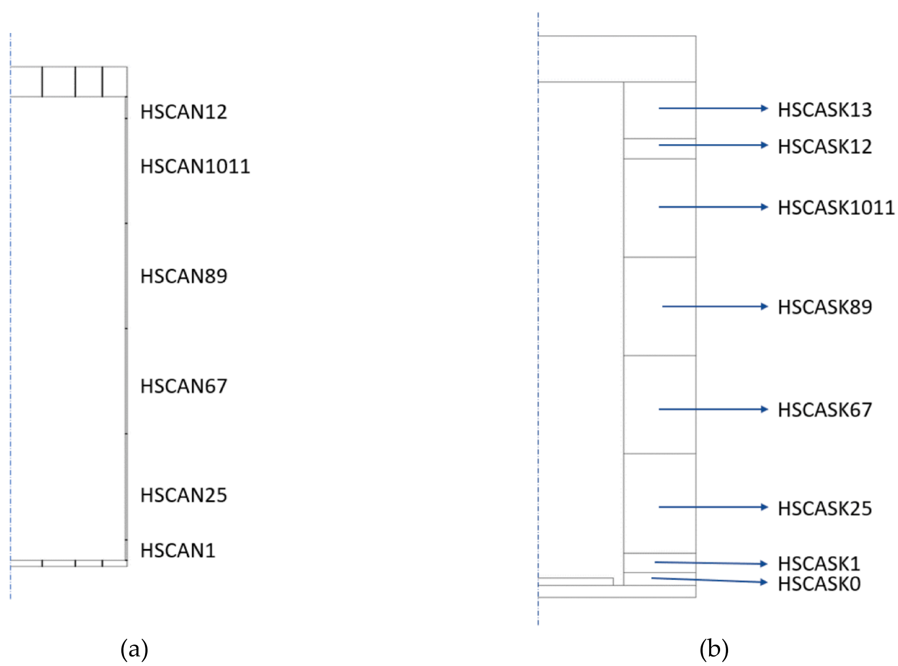

Fig. 4. Heat structures used in the modeling of MPC (a) and overpack (b) walls.

For the modeling of the off-normal conditions, the partial blockage of the air inlet has been simulated using a valve component in the inlet FP, and imposing the opening area fraction. Table 2 reports information related to the 3 addressed scenarios.

As for the accidental scenario involving the complete blockage of the air inlet, the simple nodalization employed in this work is not able to correctly reproduce the natural circulation flow that is established in the air gap when no air enters from the bottom inlets. Under this accidental circumstance, the air should be almost stationary in the lower region of the channel, whilst it should be subjected to buoyancy-driven flow in the central and upper regions. The modeling of the air channel through vertical aligned CVs with no radial splitting (as shown in Fig. 3) undermines the capability of the model to reproduce the described airflow: in particular, the simultaneously flowing of the air upward (nearby the MPC wall) and downward (close to the overpack wall) is not allowed, with the result that the model fails in simulating the proper heat extraction.

For the above-mentioned reasons, a different strategy has been adopted for the simulation of the complete blockage: using the same model employed for the partial blockage, convection was disregarded,

Table 2
Off-normal scenarios considered in the study.

Scenario	Open Inlets	Open Area
Partial Blockage 1	3 out of 4	0.174 m^2
Partial Blockage 2	2 out of 4	0.116 m^2
Partial Blockage 3	1 out of 4	0.058 m^2

while keeping active the radiation exchange. Contrary to the previous cases in which the HTC was calculated by the code itself, for the accidental scenario the HTC was user-imposed. In particular, a very low Heat Transfer Coefficient (HTC) was imposed on the external side of the MPC HSs to reproduce the conduction through the air. Exploiting the thermal-electrical analogy (Lienhard and Lienhard, 2017), it was possible to calculate the heat transfer coefficient as a function of thermal conductivity – k – and thickness of the considered layer – L:

$$HTC = \frac{k}{L}$$

Considering a value of 0.025 W/m·K for the air thermal conductivity and a value of 0.045 m for the thickness of the layer (corresponding to the distance between canister and overpack), a HTC of 0.56 W/m^2·K was calculated and employed in the simulation.

Given that the conditions employed in the present analysis are more stringent than the actual ones, it is believed that, if the calculated temperatures are below the regulatory limits, the actual temperatures in accidental condition will be too.

With regard to the adiabatic case, instead, HTC and steel emissivities were imposed equal to zero to deactivate both convective and radiative heat exchange from the canister walls.

4. Results

In the following, results for off-normal and accidental conditions in the HI-STORM 100S system are reported. However, before moving to the simulations results, it is imperative to introduce the regulatory temperature limits which cladding and concrete must comply with.

As reported in the Interim Staff Guidance-11 (U.S. NRC, 2003), allowed maximum cladding temperature is 673.15 K for long-term normal conditions. The limit is higher (843.15 K) for short-term operations and for off-normal and accidental conditions.

For the concrete in the overpack, instead, the regulatory limits are derived from ACI code 349 (ACI), with temperatures to be kept below 339 K and 366.5 K in normal and off-normal conditions, respectively. However, as reported in (HOLTEC, 2010), elevated temperature limits are allowed by the regulation if tests performed on the plain concrete employed for the HI-STORM 100S overpack show no deterioration of the concrete itself and no reduction of its density even for higher temperatures. This being the case, the temperature limits to adhere to are 422 K and 450 K in normal and off-normal conditions, respectively.

Temperature limits for both cladding and concrete are summarized in Table 3.

4.1. Off-normal scenarios

As said before, 3 different scenarios have been included in the present study for what concerns off-normal conditions:

- A partial blockage scenario with 3 (out of 4) open air inlets (hereafter called Case 1);
- A partial blockage scenario with 2 (out of 4) open air inlets (hereafter called Case 2);
- A partial blockage scenario with 1 (out of 4) open air inlets (hereafter called Case 3).

Table 3
Temperature limits for cladding and concrete.

	Normal Conditions
Cladding	673.15 K
Concrete	422 K
	Off normal and accidental conditions
Cladding	843.15 K
Concrete	450 K

Being the PCT the variable addressed in the safety regulation for the safe storage of the SNF, it has been chosen as the main target variable. For all the cases, the analysis starts with the inlet opening area being reduced. As a consequence, a raise in temperature is observable (Fig. 5). In all three cases, a new steady state is reached:

- In Case 1, the new steady state is reached more than 3.5 days after the opening area reduction by 25 %, as indicated by the vertical yellow dotted line;
- In Case 2, it is reached 4.5 days after the opening area reduction by 50 %, as indicated by the vertical red dotted line;
- In Case 3, it is reached more than 6 days after the opening area reduction by 75 %, as indicated by the vertical burgundy dotted line.

The PCT values reached at the new steady states are summarized in Table 4. In all the cases, the PCT stays below the regulatory limit. To be more precise, the temperatures do not even reach the limit for normal conditions (673.15 K).

Quantitatively speaking, the reduction in the inlet opening area seems to have only a slight influence on the PCT in Case 1 and Case 2, where a temperature raise (with respect to normal conditions) of only 3 K and 7 K is calculated, respectively. In Case 3, instead, the rise in temperature is more substantial (over 20 K). In short, it can be said that the partial blockage of the air inlet affects the PCT, to a lesser or greater extent, on the bases of the scenario severity. Nonetheless, in all of the considered off-normal scenarios, the criteria for safe storage of the SNF seem to be met.

In the attempt to characterize the increment of PCT in off-normal conditions, additional MELCOR calculations have been carried out. In particular, 5 new points have been considered: four of them have been employed to assess the raise in temperature when the percentage of air inlet blockage is between 50 % and 75 %, and a more extreme one for a 95 % air inlet blockage. As it can be seen in Fig. 6, the dataset provided by MELCOR calculations' outcomes can be approximated with a power trend. In accordance to it, in fact, a more severe raise in temperature can be observed when going over 75 % of blockage (i.e., 3 air inlets – out of 4 – are blocked and the last one is partially blocked, to different degrees).

In the same Fig., results obtained for off-normal and accidental conditions using the same FLUENT model presented in (Herranz et al., 2015) are shown. As it can be observed, there are some discrepancies, very likely attributable to different aspects. Among them, three factors may contribute the most to the observable differences:

- Code nature: MELCOR and FLUENT differ significantly in their design. MELCOR is a lumped parameter code tailored for SA scenarios, while FLUENT is a CFD code aiming for high accuracy results;
- SNF modeling approaches: FLUENT treats FAs as porous rectangular parallelepipeds with internal heat generation. In contrast, MELCOR provides a more detailed characterization of the fuel zone with integrated models;
- Air channel nodalization: as already mentioned, MELCOR employs a relatively simple nodalization for the air channel. In particular, it combines inlet and outlet openings into just two flow paths, one for air entering and one for air exiting, which may impact the simulation of off-normal scenarios.

However, despite the above-mentioned discrepancies, it is important to acknowledge that a very similar trend is observable for the results obtained from MELCOR and FLUENT calculations. In fact, also in FLUENT outcomes, the increase in temperature becomes noticeable (even more than in MELCOR) between 25 % and 50 % blockage. Moreover, just like in MELCOR, the escalation begins once the inlet blockage percentage touches 75 %.

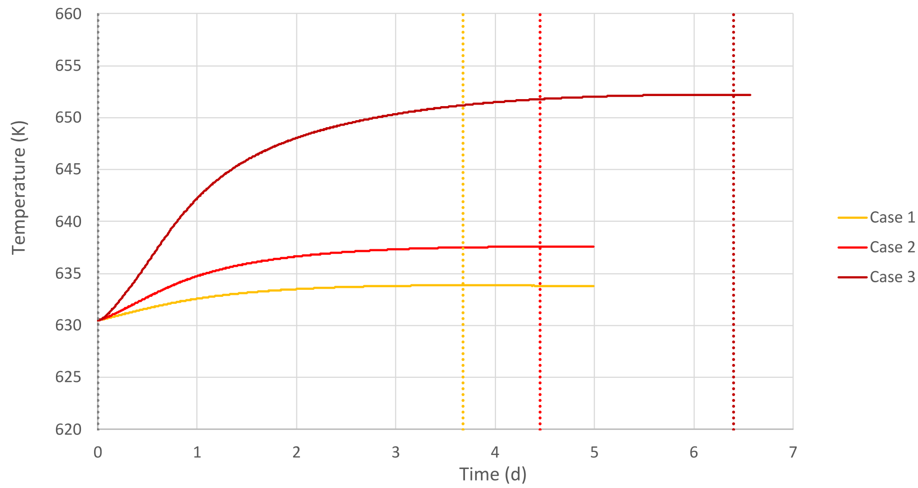

Fig. 5. PCT time evolution – off-normal scenarios.

Table 4
PCT values – off-normal scenarios.

	PCT
Case 1	633.9 K
Case 2	637.6 K
Case 3	652.2 K

For a more thorough description of the thermal behavior of the cask, the temperature radial profile (at the axial location where the PCT is attained) has been examined. Looking through Fig. 7, in which the MELCOR results for the off-normal scenarios are reported, it can be said that the trend is the same for the three considered cases, resulting quite similar to the one obtained in normal conditions (grey line). Moreover, the obtained profiles can be considered consistent with the real cask behavior. In fact:

- Temperatures decrease within the fuel zone when moving away from the center of the canister: the PCT is attained in the central FAs, whereas external FAs are colder, being closer to the Helium downcomer;
- Helium in the downcomer heats up due to the heat coming from the FAs. However, it transfers part of it to the canister wall and, indirectly, to the air in the gap;
- The thermal resistance across the steel MPC wall is almost negligible: the steel canister wall is, in fact, thin (0.013 m);
- Temperatures in the air channel are closer to the one calculated for the carbon steel liner in the internal side of the overpack wall: MELCOR calculates only an average temperature for each CV, not being able to take into account the effect of the boundary layer on velocity and temperature profiles;
- Three temperature zones can be observed in the overpack wall in agreement with the sandwich structure of the wall. At the extremities, the temperature difference in the two thin steel layers is almost indistinguishable, due to the low thermal resistance. In the middle section, the thermal resistance is higher: concrete temperature shows a jump of about 60 K in Case 1 and Case 2, and of about 70 K in Case 3.

From Fig. 7, a discussion can be started for what concerns the compliance with concrete temperature limits, as required to avoid concrete deterioration and durability. As it can be seen, concrete temperature at the axial location where the PCT is reached is below the limits (422 K and 450 K for normal and off-normal conditions, respectively) along the entire wall thickness, even for Case 3 where 75 % of the air inlet is blocked.

However, analyzing the concrete axial temperature profile, the higher temperature in the overpack is reached not in the HS corresponding to the PCT axial location (HSCASK1011), but rather on a

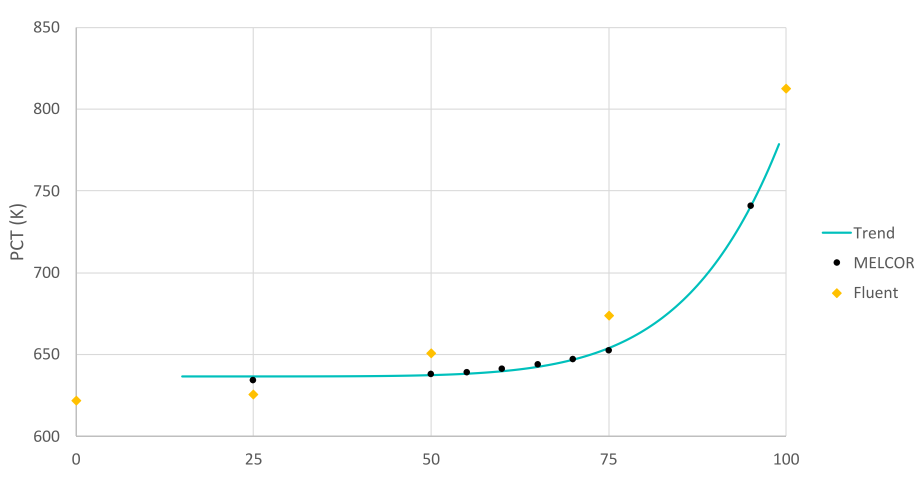

Fig. 6. PCT vs air inlet blockage %.

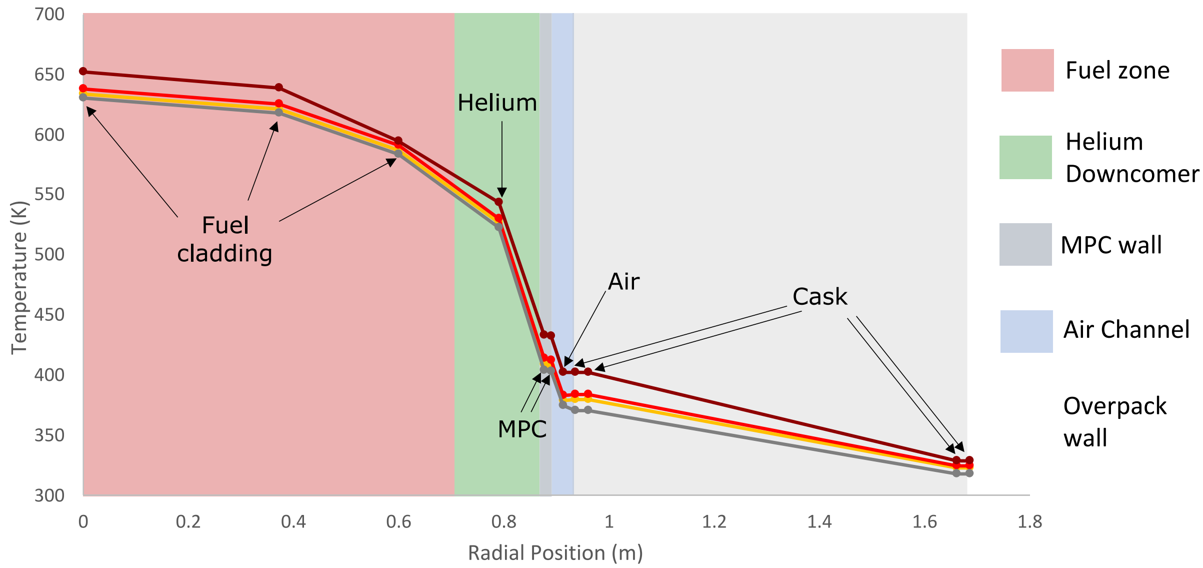

Fig. 7. Temperature radial profile (Case 1: yellow, Case 2: red, Case 3: burgundy, Normal Conditions: grey) – off-normal scenarios.

slightly higher position (HSCASK12), as shown in Figs. 8 and 9, where concrete temperatures for inner and outer side of the overpack are reported, respectively.

The concrete axial temperature profile on the inner side of the overpack is coherent with the main mechanism participating in the heat removal from the MPC. Air entering the annular gap from the bottom heats up while flowing upwards, and it transfers heat to the overpack inner wall, that, consequently, heats up following a similar trend. The same trend is also followed by the temperature profile for the outer wall of the overpack, that is cooler. In this case, although, the primary heat transfer mechanism is the conduction within the overpack wall itself. It is worth noting that temperatures stay always below regulatory limits.

4.2. Accidental scenario

As explained in Section 3, the accidental scenario involving the complete blockage of air inlet has been simulated disregarding the convective heat transfer due to the air flow in the annular channel, while keeping active the radiative exchange between MPC and overpack. In addition, a very low HTC was imposed on the external side of the MPC HSs to reproduce the conduction through the air.

For this scenario, the focus has been placed on cladding temperature, being of utmost importance to the safety of the entire system. In Fig. 10, cladding temperature for the FAs at the center of the canister is reported. As it can be observed, 8 different lines are displayed, each representing the progression in time of cladding temperature at a different axial locations (from the bottom – COR-TCL.104 – to the top – COR-TCL.111). In line with the physical behavior of the system, temperatures are lower in the lower part of the canister, and they rise when moving upwards. Moreover, it has to be highlighted that, even 7 days after the beginning of the accident, cladding temperatures are still below regulatory limits. In particular, temperature in the bottom half of the canister do not even reach the limit for normal conditions, whereas temperatures in the upper part of the fuel exceed it, but stay well below the limit for accidental conditions (843.15 K).

In addition to what commented before, when considering the maximum temperature for the cladding, it can be said that the obtained value (around 774 K) seems to be in line with the trend shown in Fig. 6. This might indicate a sort of corroboration of the strategy applied for the accidental scenario.

4.3. Adiabatic case

An entirely different situation appear when looking at the outcomes

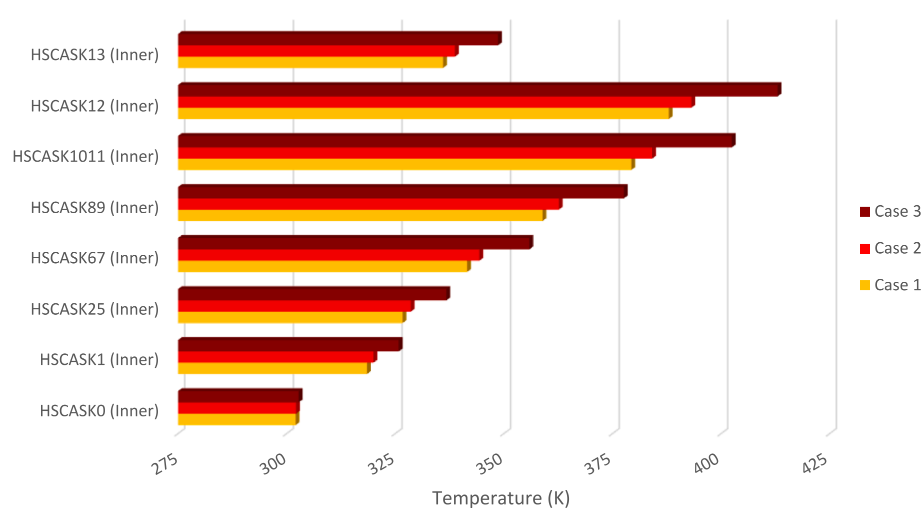

Fig. 8. Concrete axial temperature profile (overpack inner side) – off-normal scenarios.

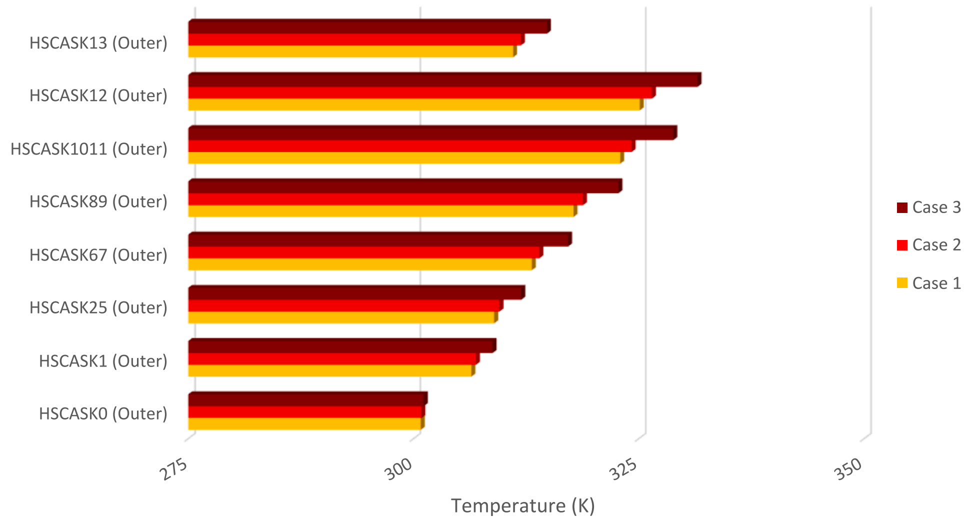

Fig. 9. Concrete axial temperature profile (overpack outer side) – off-normal scenarios.

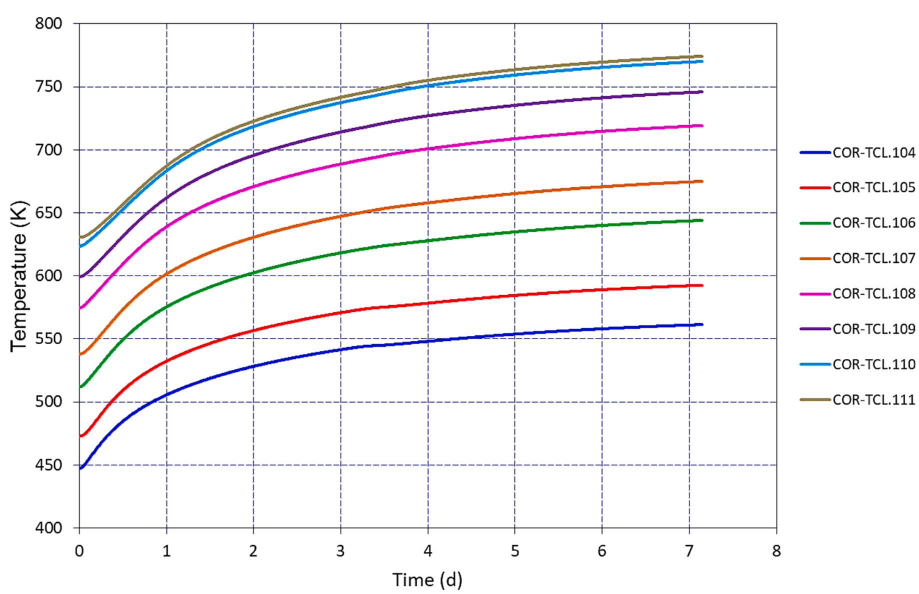

Fig. 10. Central FAs temperature at different heights – accidental scenario.

of the adiabatic case for the MPC. Even if this scenario is considered a bounding one, gathering information about the escalation of temperatures could help for a timely intervention in the accident management.

As it can be seen in Fig. 11, in this extreme case the issue is not whether the limits are exceeded or not, but rather how long before they are exceeded. With this in mind, few observations can be done about the timeline of the accident progression:

- After little more than 9 h, temperatures in the upper part of the central FAs exceed the 1st limit (that is the one for normal conditions);
- After about 33 h, temperatures in the upper part exceeds also the 2nd limit (that is the one for off-normal and accidental conditions);
- After 2 d, the central FAs have temperatures above the 1st limit in all the axial locations;
- After 3 d, temperatures are above the 2nd limit, and PCT exceeds 1000.0 K.

To have a further and better visualization of the temperature progression within the "core" of the cask, temperatures are reproduced by means of heatmaps (Fig. 12). Levels represent axial elevations, whereas rings delineate the radial location of the FAs, with Ring 1 containing central (and hotter) FAs and Ring 3 including the external (and colder) ones.

As it can be noticed, with the progressing in time of the accident, there is a progressive homogenization of the temperature within the canister, particularly in the upper half of the FAs, where higher temperatures are hit.

Furthermore, a down-shifting of axial location of the PCT is observable: in normal conditions (t_0) the highest temperature is reached in the 11th level, whereas it moves first in the 10th level and then to the 9th when advancing in time. This is compatible with what observed in (Li and Liu, 2016), where a similar down-shifting in the PCT was obtained from a FLUENT calculation for a complete blockage of air inlet. The phenomenon is very likely correlated with two concurrent circumstances: the continuous heat production from the SNF on one side, and the worsening of the heat extraction on the other. While these circumstances led to a gradual homogenization of the temperature within the MPC, the central region is the hottest one. This is imputable to the limited cooling possibilities: in short, FAs in the central region are

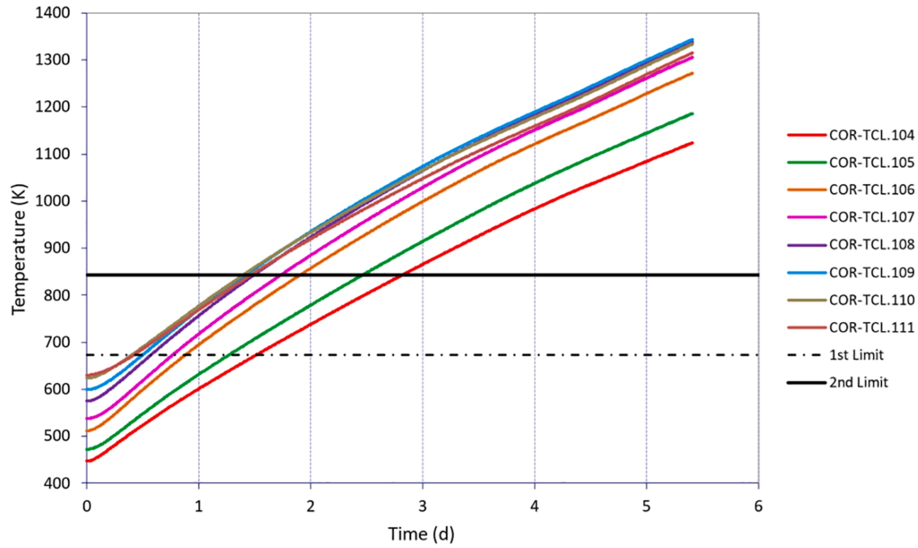

Fig. 11. Central FAs temperature at different heights - adiabatic case.

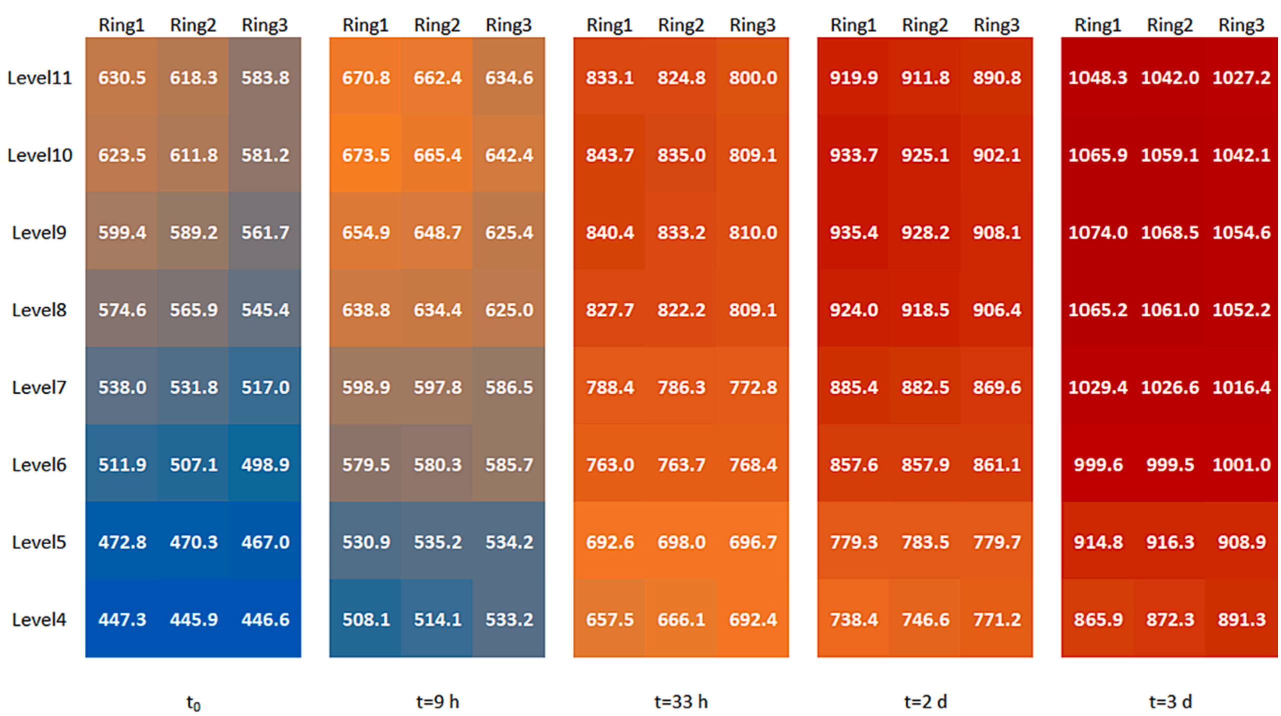

Fig. 12. Temperature (K) progression in the "core" region - adiabatic case.

surrounded by other FAs of comparable high temperature. Additionally, also the Helium flowing through the FAs retains high temperatures due to the unavailable heat dissipation to the air channel.

5. Summary and conclusions

In this paper, the efforts made in the evaluation of the performance of a concrete-based DCS in off-normal and accidental conditions are reported. Particular attention has been paid to the assessment of the influence of out-of-the-ordinary scenarios on the PCT, that is the target variable for a safety evaluation. Moreover, overpack concrete temperature compliance with the regulatory limits has been investigated in order to preserve concrete integrity and its shielding function.

Several scenarios have been simulated for the HI-STORM 100S system, with the MELCOR code (version 2.2.18019). In this regard, the present study serves an additional scope: to further testing MELCOR, that is a code developed for the analysis of SA scenarios, outside its natural domain of application.

Achieved results allow to draw some conclusions:

- Off-normal conditions have been simulated considering a partial blockage of the air inlet openings at the bottom of the overpack. In particular, three scenarios with growing intensity have been studied, with an inlet area reduction of 25 %, 50 % and 75 %, respectively.

  The partial blockage of the air inlet opening seems to affect the PCT, to a lesser or greater extent, on the bases of the scenario severity. However, the criteria for safe storage of the SNF seem to be ensured in all the considered off-normal scenarios. The PCT, in fact, stays below the regulatory limit and does not even reach the limit for normal conditions (673.15 K).

Even the analysis of concrete temperatures reveals that temperature limits are not exceeded. In addition, obtained axial temperature profiles (for both inner and outer side of the overpack) show that MELCOR outcomes are consistent with the main mechanisms driving the heat transfer (and extraction) from the system.

- As for the accidental scenario, a complete blockage of air inlet has been considered. In this case, the simple air channel nodalization employed in the MELCOR model was not able to correctly reproduce the natural circulation that is established in the air gap. For this reason, the accidental scenario has been simulated in a slight different way: disregarding the convective heat transfer due to the air flow in the annular channel, while keeping active the radiative exchange between MPC and overpack. In addition, conduction through air has been reproduced imposing a very low HTC on the external side of the canister HSs.

  Results show that, even after 7 days after the beginning of the accident, cladding temperatures are still below regulatory limits. Even in this case, the cooling capacity of the DCS is maintained.
- As a further step in the thermal and safety assessment, an adiabatic case for the MPC was additionally explored.

  The outcomes from this extreme case are definitely different from the previous cases. Temperature limits are, in fact, not met, and it takes less than 10 h for the first limit to be exceeded. In less than 2 d, PCT exceeds also the 2nd limit, reaching 1000 K in around 3 d. Additionally, it can be observed an homogenization of the temperatures within the canister, with a down-shifting of the PCT axial position.

In short, it can be said that temperatures calculated in the considered off-normal and accidental scenarios are below the allowable values. This means that the cooling and the safe storage of the SNF seem to be ensured also in out-of-the ordinary situations.

For what concerns bounding conditions (such as the ones involved in the adiabatic case), instead, the temperature progression in time is of utmost importance for any accident management action to be taken. Results suggest that a tempestive response should be considered for the safety of SNF not to be at risk.

Furthermore, the MELCOR code has shown good adaptability and flexibility, being able to reproduce off-normal and even more extreme scenarios. Nonetheless, it has also shown some limitations, in particular for what concerns the simulation of the natural circulation in the air channel when the most severe accidental conditions occur.

Based on the preceding discussion, the present research could be further developed following two main directions. The first one involves continuing on the simulation path: while the present study addresses scenarios related to the partial to complete blockage of the air inlet, it is important to extend the range of accidental scenarios under investigation (i.e., fire and Helium leakage). By doing so, a more comprehensive understanding of the system response under different circumstances could be provided. On the other side, it is fundamental to consider the limitations related to the simulation of the natural circulation. To this aim, a more complex nodalization for the air channel should be developed and tested. In fact, by means of a refined nodalization, the understanding of the air channel dynamics could be improved, and its influence on the entire system better investigated.

CRediT authorship contribution statement

Michela Angelucci: Conceptualization, Formal analysis, Methodology, Software, Writing – original draft, Writing – review & editing. **Luis E. Herranz:** Conceptualization, Supervision, Writing – review & editing. **Sandro Paci:** Conceptualization, Funding acquisition, Supervision, Writing – review & editing.

Declaration of competing interest

The authors declare that they have no known competing financial interests or personal relationships that could have appeared to influence the work reported in this paper.

Data availability

Data will be made available on request.

References

ACI, n.d.. ACI CODE 349-13: Code Requirements for Nuclear Safety-Related Concrete Structures and Commentary.

Angelucci, M., Herranz, L.E., Paci, S., 2021. Thermal analysis of HI-STORM 100S dry cask with the MELCOR code. J. Phys. Conf. Ser. 1868 https://doi.org/10.1088/1742-6596/1868/1/012001.

Angelucci, M., Paci, S., Feria, F., Herranz, L.E., 2022. Uncertainty and sensitivity analysis of a dry cask for spent nuclear fuel. Energies. https://doi.org/10.3390/en15031216.

Ansys Inc. ANSYS Fluent User's Guide.

Ansys Inc. ANSYS CFX-Solver Theory Guide.

Bang, K.S., Yu, S.H., Lee, S.H., Lee, J.C., Seo, K.S., 2014. Experimental investigation of heat removal performance of a concrete storage cask. Ann. Nucl. Energy 85, 679–686. https://doi.org/10.1016/j.anucene.2015.06.024.

Benavides, J., Jimenez, G., Galbán, M., Lloret, M., 2019. Methodology for Thermal Analysis of Spent Nuclear Fuel Dry Cask Using CFD Codes. Ann. Nucl. Energy 133, 257–274. https://doi.org/10.1016/j.anucene.2019.05.026.

Bunn, M., Holdren, J.P., Macfarlane, A., Pickett, S.E., Suzuki, A., Suzuki, T., Weeks, J., 2001. Interim Storage of Spent Nuclear Fuel: A Safe, Flexible, and Cost-Effective Approach to Spent Fuel Management Citation Terms of Use Share Your Story.

Herranz, L.E., Penalva, J., Feria, F., 2015. CFD analysis of a cask for spent fuel dry storage: model fundamentals and sensitivity studies. Ann. Nucl. Energy 76, 54–62. https://doi.org/10.1016/j.anucene.2014.09.032.

Humphries, L.L., Beeny, B.A., Gelbard, F., Louie, D.L., Phillips, J., Schmidt, R.C., Bixler, N.E., 2021. MELCOR Computer Code Manuals, Vol. 1:. Primer and Users' Guide.

HOLTEC, I., 2010. Final Safety Analysis Report (FSAR) for the HI-STORM 100 Cask System.

Humphries, L.L., Beeny, B.A., Gelbard, F., Haskin, T., Louie, D.L., Phillips, J., Schmidt, R. C., Bixler, N.E., 2021. MELCOR Computer Code Manuals, Vol. 2: Reference Manual, Version 2.2.18019.

IAEA, 2002. LONG TERM STORAGE OF SPENT NUCLEAR FUEL - SURVEY AND RECOMMENDATION.

Lee, J.-C., Kim, D.-H., Bang, K.-S., Seo, K.-S., Choi, B.-I., Lee, H.-Y., 2005. Thermal Analysis of a Storage Cask for 24 Spent PWR Fuel Assemblies. Packag. Transp. Storage Secur. Radioact. Mater. 16, 19–26. https://doi.org/10.1179/174650905775295611.

Li, J., Liu, Y.Y., 2016. Thermal modeling of a vertical dry storage cask for used nuclear fuel. Nucl. Eng. Des. 301, 74–88. https://doi.org/10.1016/j.nucengdes.2016.01.008.

Lienhard, J.H.I., Lienhard, J.H.V., 2017. A Heat Transfer Textbook (fourth edition).

Nourgaliev, R.R., Christon, M.A., Bakosi, J., Lowrie, R.B., Pritchett-Sheats, L.-TH., 2013. A Thermal-Hydraulics Code for Nuclear Reactor Applications. Proc. 15th Int. Top. Meet. Nucl. React. Therm. - Hydraul. 33.

Penalva, J., Feria, F., Herranz, L.E., 2017. Thermal performance of a concrete cask: methodology to model helium leakage from the steel canister. Ann. Nucl. Energy 108, 229–238. https://doi.org/10.1016/J.ANUCENE.2017.04.049.

Penalva, J., Feria, F., Herranz, L.E., 2021. Modeling maximum fuel temperature in dry storage: from the cfd analysis to the engineering approach. Nucl. Eng. Des. 383, 111435 https://doi.org/10.1016/j.nucengdes.2021.111435.

Poskas, P., Smaizys, A., Simonis, V., 2006. Radiological and thermal characteristics of CASTOR RBMK-1500 and CONSTOR RBMK-1500 casks for spent nuclear fuel storage at ignalina nuclear power plant. Kerntechnik 71, 222–227. https://doi.org/10.3139/124.100297/MACHINEREADABLECITATION/RIS.

Ratiko, R., Sumarbagiono, R., Aisyah, A., Wati, W., Heriyanto, K., Mirawaty, M., Artiani, P.A., Purwanto, Y., Saputra, D.L.I., Rachmadetin, J., et al., 2022. Theoretical and experimental analysis on influence of natural airflow on spent fuel heat removal in dry cask storage. Sustain. 14 https://doi.org/10.3390/su14031859.

Rector, D., Cuta, J., Lombardo, N., 1986. COBRA-SFS Thermal-Hydraulic Analysis of the CASTOR-1C and REA 2023 BWR Storage Casks Containing Consolidated Spent. Fuel. NL-5802.

Šimonis, V., Ragaišis, V., Šmaizys, A., 2013. Thermal Assessment of New Ignalina NPP Casks for Spent Nuclear Fuel Storage at Some Abnormal Conditions. Mechanika 19, 159–166. https://doi.org/10.5755/j01.mech.19.2.4153.

SIEMENS. STAR CCM+.

U.S. NRC, 2003. Interim Staff Guidance-11, Revision 3 Issue: Cladding Considerations for the Transportation and Storage of Spent Fuel.

U.S. NRC. PART 72 — LICENSING REQUIREMENTS FOR THE INDEPENDENT STORAGE OF SPENT NUCLEAR FUEL, HIGH-LEVEL RADIOACTIVE WASTE, AND REACTOR-RELATED GREATER THAN CLASS C WASTE | NRC.Gov.

U.S. NRC, 2010. Standard Review Plan for Spent Fuel Dry Storage Systems at a General License Facility Final Report Office of Nuclear Material Safety and Safeguards, NUREG-1536.

U.S. NRC, 2013. Computational Fluid Dynamics Best Practice Guidelines for Dry Cask Applications. p. NUREG-2152.

Wang, Y.H., Lin, Y.P., Chang, H.Y., Lai, C.M., 2021. Ventilation pattern and heat dissipation characteristics of a vertical dry storage cask for spent nuclear fuel: wind tunnel experiments and CFD simulations. Ann. Nucl. Energy 160, 108364. https://doi.org/10.1016/j.anucene.2021.108364.

Wu, Y., Klein, J., Zhou, H., Zuo, L., 2018. Thermal and fluid analysis of dry cask storage containers over multiple years of service. Ann. Nucl. Energy 112, 132–142. https://doi.org/10.1016/J.ANUCENE.2017.10.013.